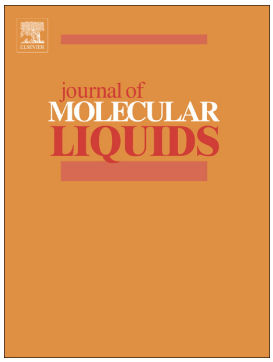


# Bichromophoric pyrazoline derivative with solvent-selective photoluminescence quenching

Andreea L. Chibac, Gheorghe Roman, Corneliu Cojocaru, Sergiu Shova, Gabriela Sacarescu, Mihaela Simionescu, Liviu Sacarescu

PII: S0167-7322(18)33190-8
DOI: https://doi.org/10.1016/j.molliq.2019.01.067
Reference: MOLLIQ 10298

To appear in: *Journal of Molecular Liquids*

Received date: 21 June 2018
Revised date: 7 December 2018
Accepted date: 12 January 2019

Please cite this article as: Andreea L. Chibac, Gheorghe Roman, Corneliu Cojocaru, Sergiu Shova, Gabriela Sacarescu, Mihaela Simionescu, Liviu Sacarescu , Bichromophoric pyrazoline derivative with solvent-selective photoluminescence quenching. Molliq (2019), https://doi.org/10.1016/j.molliq.2019.01.067

# Bichromophoric Pyrazoline Derivative with Solvent-Selective Photoluminescence Quenching

Andreea L. Chibac, Gheorghe Roman, Corneliu Cojocaru, Sergiu Shova, Gabriela Sacarescu, Mihaela Simionescu, Liviu Sacarescu*

Petru Poni Institute of Macromolecular Chemistry, 41 A Grigore Ghica Voda Alley, 700487, Iasi, Romania

*e-mail: livius@icmpp.ro

**Abstract**

The quenching of fluorescence in the presence of chloromethanes, which is an unprecedented effect for pyrazolines, has been evidenced for the first time in the case of 1,3-diphenyl-5-{4-[(4-vinylbenzyl)oxy]phenyl}-4,5-dihydropyrazole. The detailed synthesis of this aryl trisubstituted pyrazoline that combines two chromophoric units in a non-conjugated manner is presented. The compound has been extensively characterized from a structural point of view, and its crystal structure has been determined by single crystal X-ray crystallography. The fluorescence study has evidenced the particular behavior of this pyrazoline derivative in solutions of chloromethanes, and the insight gained from the experimental data has been useful in elaborating a plausible fluorescence quenching mechanism. The investigated compound was modeled by Density Functional Theory (DFT) to point out the particularities of the electron transitions in gas phase as well as in the implicit solvents. Also, the HOMO-LUMO energy gap, mapped electrostatic potential, electronic density, dipole moment and polarizability have been reported for the pyrazoline derivative.

**Keywords:** Pyrazoline; Synthesis; Bichromophore; Fluorescence; Quenching; Molecular modelling

## 1. Introduction

An ever-growing research field is represented by sensors that could be used to supervise various activities and processes, or even to monitor the health status of human beings [1,2]. From this point of view, important efforts are concerned with light sensing and response of materials or living organisms under light irradiation [3]. Fluorescence sensing is already a well-known technique with particular applications in chemistry and biology [4]. This method is highly versatile, and its resolution down to molecular level is extremely useful in molecular imaging [5]. To date, there are a huge number of organic molecules that were reported as valuable fluorophores with different optical properties and sensing capabilities [6]. An interesting class of compounds is represented by pyrazoles and their derivatives. In the case of these compounds, several additional useful properties have been described beside fluorescence. One of these applications refers to these compounds' utility as active compounds in the therapy of various medical conditions [7]. Thus, both optical and bio-active properties could be combined in the same chemical structure to provide important advantages, especially when the effect of the treatment should be monitored locally.

It is known that pyrazolines allow characteristic intramolecular charge transfer effects that generate properties useful for various applications [8,9]. Particularly, 1,3,5-triaryl-2-pyrazoline derivatives that possess fluorescence in the blue region of the spectrum have been employed also as hole transporting materials, organic electroluminescent devices, fluorescent probes for chemosensors and fluorescent switches [10]. In all of these examples, pyrazolines have been reported as ligands in complex metal-organic systems in which the nature of the cation is crucial to the materialization of the desired property [11,12].

This paper describes a pyrazoline having specific properties, distinctive than those reported for other members of the class. Hence, 1,3-Diphenyl-5-{4-[(4-vinylbenzyl)oxy]phenyl}-4,5-dihydropyrazole has a bichromophoric structure that enables a selective blue emission as a function of the solvent employed. Thus, fluorescence measurement experiments conducted for this pyrazoline in chloromethanes as solvents have resulted in quenching, whereas the same pyrazoline exhibits a strong emission and a quantic yield higher than 75% in various other polar and non-polar solvents. This selectivity could be exploited for the development of detection sensors that operate through fluorescence quenching, and are effective for the identification, monitoring and eventually treatment of medical conditions for which the local modification of chemical composition of the tissue is indicative.

## 2. Experimental

### *2.1. Materials, methods and instrumentation*

All the chemical reagents and solvents were obtained from Sigma–Aldrich (Schnelldorf, Germany) and were used without prior purification. The optical studies were performed using UV-grade solvents. Melting points were taken on a MEL-TEMP capillary melting point apparatus and are uncorrected. Elemental analysis was conducted on a PerkinElmer 2400 Series II CHNS/O system. $^{1}$H and $^{13}$C NMR spectra were recorded on a Bruker Avance 400-MHz spectrometer. The signals owing to residual protons in the deuterated solvents were used as internal standards for the $^{1}$H NMR spectra. The chemical shifts for the carbon atoms are given relative to deuteriochloroform ($\delta$ = 77.16 ppm) and DMSO-$d_6$ ($\delta$ = 39.52 ppm). Fourier Transform-Infrared (FT-IR) spectra were taken on a FT-IR Bruker Vertex 70 instrument in transmission mode, using KBr pellets. The UV-Vis absorption spectrum was recorded on a SPECORD 210 Plus Analytik Jena spectrophotometer. Fluorescence spectra were collected on a Perkin-Elmer LS 55 spectrofluorometer. Single crystal X-ray measurements were carried out using Oxford–Diffraction XCALIBUR E CCD equipment set up with graphite–monochromated Mo–Kα radiation.

### *2.2. Chemistry*

#### *2.2.1. Synthesis of 4-[(4-vinylbenzyl)oxy]benzaldehyde **1***

To a solution of KOH (658 mg, 10 mmol, 85% purity) in ethanol 96% (10 mL), 4-hydroxybenzaldehyde (1.22 g, 10 mmol) was added, and then the mixture was stirred at room temperature for 5 min. 4-Vinylbenzyl chloride (1.694 mg, 10 mmol, 90% purity) was then added, and then the reaction mixture was heated at reflux temperature for 2 h. Aqueous 5% KOH (2 mL) was then gradually added to the hot mixture, followed by water (30 mL), and the mixture was further stirred for 30 min. The resulting solid was filtered, air-dried, and recrystallized to give colorless crystals (1.71 g, 72%), mp 76–77 °C (methanol). $^{1}$H NMR ($CDCl_3$, 400 MHz): $\delta$ 5.14 (s, 2H), 5.28 (d, $J$ = 10.4 Hz, 1H), 5.78 (d, $J$ = 17.6 Hz, 1H), 6.73 (dd, $J$ = 10.4 and 17.6 Hz, 1H), 7.07 (d, $J$ = 8.4 Hz, 2H), 7.39 (d, $J$ = 8.0 Hz, 2H), 7.45 (d, $J$ = 8.0 Hz, 2H), 7.84 (d, $J$ = 8.4 Hz, 2H), 9.89 (s, 1H). $^{13}$C NMR ($CDCl_3$, 100 MHz): $\delta$ 70.2, 114.6, 115.3, 126.7, 127.8, 130.3, 132.1, 135.5, 136.4, 137.8, 163.8, 190.9. *Anal.* Calcd. for $C_{16}H_{14}O_2$: C 80.65; H 5.92. Found: C 80.41; H 5.73.

#### *2.2.2. Synthesis of (E)-1-phenyl-3-{4-[(4-vinylbenzyl)oxy]phenyl}prop-2-en-1-one **2***

4-[(4-Vinylbenzyl)oxy]benzaldehyde **1** (1428 mg, 6 mmol) was dissolved in warm methanol (60 mL) with efficient stirring. The solution was cooled to room temperature, then acetophenone (720 mg, 6 mmol) and 10% NaOH (1 mL) were sequentially added. The mixture was stirred at room temperature overnight, then the solid that had separated was filtered, washed sequentially with 2-propanol (2× 10 mL) and water (2× 10 mL), air-dried, and recrystallized to afford yellowish leaflets (1080 mg, 53%), mp 104–105 °C (methanol). $^{1}$H NMR ($CDCl_3$, 400 MHz): $\delta$ 5.10 (s, 2H), 5.28 (d, $J$ = 10.4 Hz, 1H), 5.78 (d, $J$ = 17.6 Hz, 1H), 6.73 (dd, $J$ = 10.4 and 17.6 Hz, 1H), 7.01 (d, $J$ = 8.4 Hz, 2H), 7.36–7.47 (m, 5H), 7.47–7.55 (m, 2H), 7.55–7.64 (m, 3H) 7.79 (d, $J$ = 15.6 Hz, 1H), 8.02 (d, $J$ = 7.2 Hz, 2H). $^{13}$C NMR ($CDCl_3$, 100 MHz): $\delta$ 70.0, 114.4, 115.4, 120.0, 126.6, 127.8, 128.0, 128.5, 128.7, 130.4, 132.7, 136.0, 136.5, 137.7, 138.6, 144.7, 160.9, 190.7. *Anal.* Calcd. for $C_{24}H_{20}O_2$: C 84.68; H 5.92. Found: C 84.40; H 6.15.

*2.2.3. Synthesis of 1,3-diphenyl-5-{4-[(4-vinylbenzyl)oxy]phenyl}-4,5-dihydro-1H-pyrazole **3***

To a solution of (*E*)-1-phenyl-3-(4-([4-vinylbenzyl]oxy)phenyl)prop-2-en-1-one **2** (1020 mg, 3 mmol) in glacial acetic acid (20 mL), phenylhydrazine (432 mg, 4 mmol) is added. The solution is stirred at room temperature overnight, then the solid that separated was filtered, washed with ethanol (2× 10 mL), air-dried and recrystallized twice from ethyl acetate–2-propanol (1:3, v/v) to afford off-white crystals (465 mg, 36%), mp 139–140 °C. FTIR (KBr, $\nu_{max}$ [$cm^{-1}$]): 685s, 747s, 824s, 987m, 1052m, 1129s, 1172m, 1216m, 1242vs, 1329m, 1390s, 1496vs, 1587vs, 1656w, 2835w, 2852w, 2885w, 2911w, 2921w, 2976w, 3027m, 3035m, 3052m, 3067w, 3129w. $^{1}$H NMR (DMSO-$d_6$, 400 MHz): $\delta$ 3.07 (dd, $J$ = 6.0 and 13.2 Hz, 1H), 3.86 (dd, $J$ = 12.0 and 13.2 Hz, 1H), 5.03 (s, 2H), 5.25 (d, $J$ = 11.2 Hz, 1H), 5.41 (dd, $J$ = 6.0 and 12.0 Hz, 1H), 5.83 (d, $J$ = 18.0 Hz, 1H), 6.66–6.79 (m, 2H), 6.96 (d, $J$ = 8.8 Hz, 2H), 7.02 (d, $J$ = 8.0 Hz, 2H), 7.10–7.18 (m, 2H), 7.21 (d, $J$ = 8.8 Hz, 2H), 7.32–7.51 (m, 7H), 7.74 (d, $J$ = 7.6 Hz, 2H), $^{13}$C NMR (DMSO-$d_6$, 100 MHz): $\delta$ 43.0, 62.6, 68.9, 113.0, 114.5, 115.2, 118.6, 125.7, 126.2, 127.1, 128.0, 128.7, 128.9, 132.4, 134.7, 136.3, 136.7, 144.3, 147.2, 157.6. *Anal.* Calcd. for $C_{30}H_{26}N_2O$: C 83.69; H 6.09; N 6.51. Found: C 83.44; H 6.17; N 6.33.

*2.3. Single-crystal X-ray diffraction study*

A single-crystal of pyrazoline **3**, which has been obtained through the slow diffusion of methanol into a solution of the compound in dichloromethane, was used for the

crystallographic data collection. The unit cell estimation and data integration were done using the CrysAlis package of Oxford Diffraction [13]. The molecular structure was solved by direct methods using Olex2 program [14] and refined by full-matrix least-squares on $F^2$ with SHELXL-97 [15]. The molecular-structure plot was rendering by Olex2 software.

*2.4. UV-Vis and fluorescence measurements*

The absorption spectrum of compound **3** was recorded either in toluene or chloroform solutions at room temperature, using 10 mm quartz cells. The absorption maximum of pyrazoline **3** was used as excitation wavelength ($\lambda$ = 365 nm) for all fluorescence spectra. The excitation slits were set at 15 and 0 nm for the measurements in toluene and DMSO solutions, respectively. Due to the weak fluorescence emission the measurements in chloroform and carbon tetrachloride, were done by amplifying the signal with the excitation slits set at 5 and 8 nm. The concentration of compound **3** in each solvent was $5\times10^{-3}$ wt%. In toluene and chloroform, the fluorescence spectra were recorded at different concentrations in the range of $10^{-4}$–$5\times10^{-2}$ wt%. For the quenching experiment using the toluene solution of pyrazoline **3**, the quencher concentration of chloroform was varied in the range 0.0 to 23.33 wt%.

*2.5. Molecular modeling*

All computations were done using the Gaussian09 [16] software package on a Dell server with 24 computing cores. Molecular modeling results were analyzed in GaussView 5 graphical-interface program [17] running on a Dell Precision workstation T7910. Density functional theory (DFT) methods (B3LYP and CAM-B3LYP) were employed for the molecular modeling using split-valence basis sets. The geometry optimization of the investigated molecule was done by minimizing the energy with respect to all geometrical parameters without imposing any symmetry constrains. The input structure for optimization was taken from the CIF-file derived from X-ray single-crystal measurements. Subsequently, the geometry optimization assisted by frequency calculation was performed on a single molecule in gas phase. All optimized geometries resulted out of different basis sets unveiled $C_1$ point group and no imaginary frequencies, thereby confirming the minimum-energy structures. The electronic absorption spectra of pyrazoline **3** were predicted by the time-dependent density functional theory (TD-DFT). In addition, the YASARA program [18] was employed for conformational analysis and explicit solute-solvent interaction simulation.

## 3. Results and Discussion

A fluorescent pyrazoline having a vinyl moiety has been synthesized with the intention to develop new fluorescence sensors (Scheme 1). The vinyl moiety at position 5 of the designed pyrazoline has been put in place using commercially available 4-vinylbenzyl chloride, which was reacted with 4-hydroxybenzaldehyde under the conditions of Williamson ether synthesis (Scheme 1). Next, Claisen-Schmidt condensation of the resulting vinyl-containing aldehyde **1** with acetophenone was conducted in a large volume of methanol, in the presence of catalytic amounts of NaOH, to afford the intermediate chalcone **2**, which led to the desired pyrazoline **3** upon condensation with phenylhydrazine in acetic acid in the final step of the reaction sequence. A similar synthetic strategy has been used by Qi *et al.* for the preparation of the same compound [19].

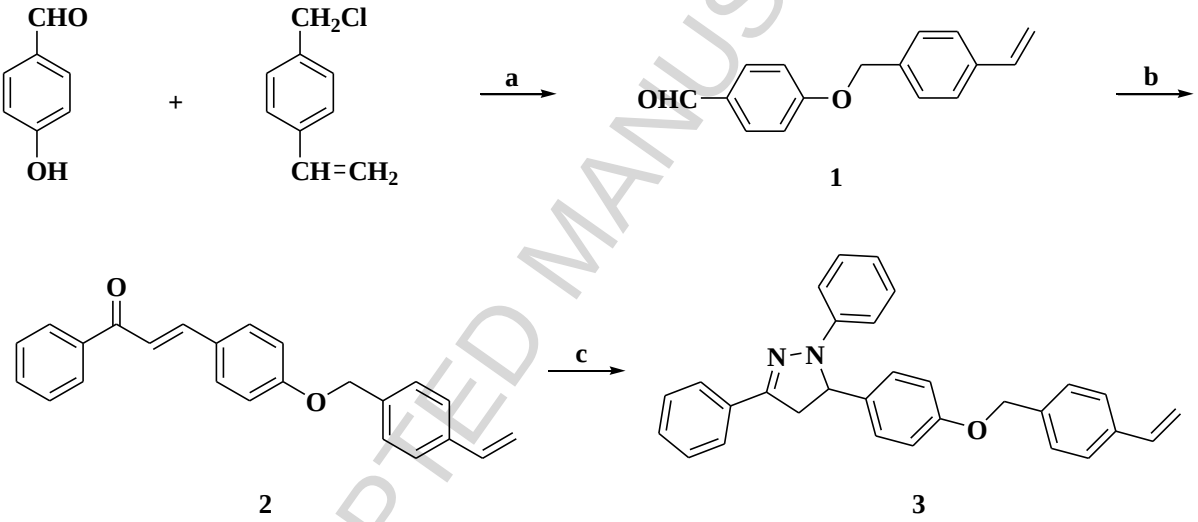


Scheme 1. Synthesis of fluorescent pyrazoline **3**. Reactants and conditions: (a) ethanol 96%, KOH, reflux, 2 h; (b) acetophenone, methanol, NaOH, room temperature, 18 h; (c) phenylhydrazine, glacial acetic acid, room temperature, 18 h.

Aldehyde 1 is a known compound, whose synthesis from the same starting materials has been reported using several approaches, and the NMR characteristics of this compound, which have been only recently fully described [19-23], are in agreement with those previously reported. To the best of our knowledge, compounds 2 and 3 have only been mentioned once in the literature [19], although pyrazoline 3 appears to have been previously employed also as a fluorescent model drug to investigate the internalization of aggregates of an amphiphilic copolymer by cells [24]. Careful duplication of the procedure previously reported [19] has led in our hands to the isolation of a mixture of unreacted starting material

and reaction product. Nevertheless, the extension of the reaction time up to 18 h allowed the separation of a crude material consisting mostly of the desired compound, from which pyrazoline 3 was obtained in pure form only after repeated recrystallizations, which occurred with significant loss of material and lowered the yield.

The structure of the target compound 3 has been established by NMR spectroscopy. The proton spectrum of pyrazoline 3 has been previously described [19], but no comments on its characteristics have been provided. The structure of pyrazoline 3 was confirmed through the identification of the three doublets of doublets centered at 3.07, 3.86 and 5.41 ppm, corresponding to the protons at C-4 and C-5 of the pyrazoline ring. Formation of pyrazoline 3 has been also substantiated through the presence of two peaks in the aliphatic region of the 13C NMR spectrum of this compound, corresponding to C-4 (43.0 ppm) and C-5 (63.6 ppm).

The synthesized pyrazoline **3** afforded single crystals upon slow diffusion of methanol into its solution in dichloromethane. They were further analyzed using X-ray diffraction to obtain the crystallographic data and refinement details presented in ESI Table S1.

The molecular structure observed for pyrazoline **3** is shown in Figure 1. The supramolecular packing structure was formed through CH…π-aromatic interactions pointed out by hydrogen-to-centroid distance ranging from 2.724 Å to 3.025 Å (ESI, Fig. S1).

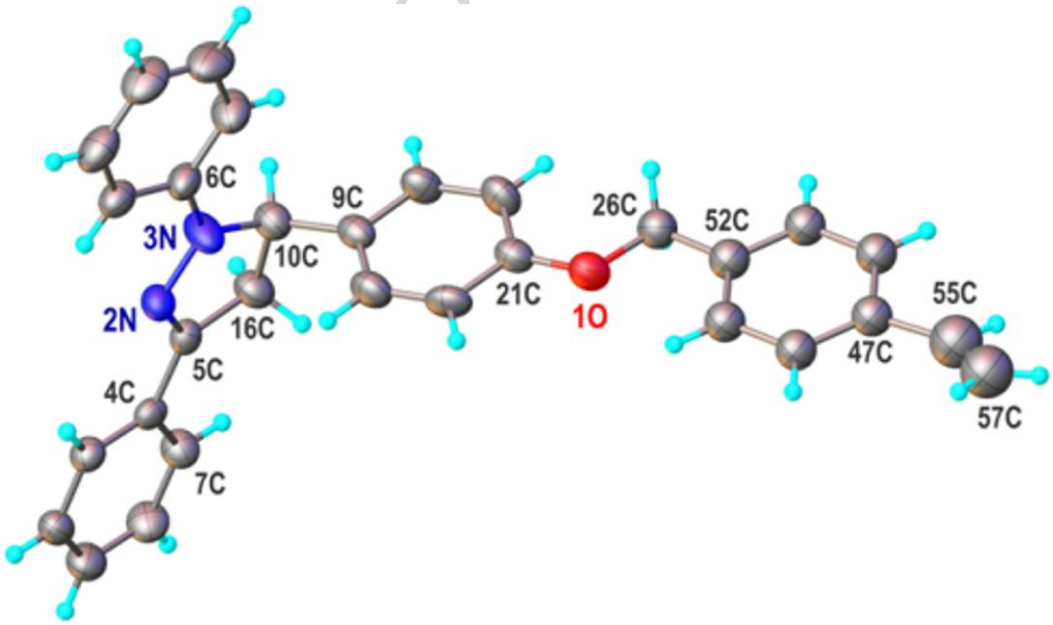


Figure 1. Molecular structure of pyrazoline **3** resulted from single crystal X-ray structure analysis (Olex2 view), thermal ellipsoids drawn at 50% probability level.

UV-Vis and fluorescence (FL) spectra of pyrazoline **3** in either chloroform or toluene are presented in Figure 2. Any attempt to interpret the UV-Vis spectrum of pyrazoline **3** has to consider the particular structure of this compound, which consists of two chromophores represented by the two separate, uncoupled conjugated electronic systems [20,26]. One of the chromophores (**C1**) is represented by the phenyl groups connected through the hydrazone bridge within the pyrazoline core, and the other (**C2**) is the vinylbenzyloxyphenyl substituent at position 5 of the pyrazoline ring. Consequently, two different electron transitions correlated with these conjugated systems should be present in the UV-Vis spectrum of pyrazoline **3** (Fig. 2a). These electronic transitions can be best observed when the UV absorption spectrum of pyrazoline **3** is recorded in chloroform. One of them is located at 260 nm, and it was assigned to the π-π* electronic transitions in the **C2** system. The other UV absorption peak is noticeable around 362 nm, and it was associated with the π-π*electron transitions in the **C1** chromophore. Due to the solvent cut-off, the UV spectrum of pyrazoline **3** in toluene displayed only the **C1** peak, which is located also at 362 nm. Moreover, the position, the intensity, and even the shape of the UV absorption band assigned to the pyrazoline core (**C1**) are not affected by the nature of the solvent, which suggests that the **C1** ground state is not perturbed in any solvent, whether the solvent is either mostly non-polar (toluene) or slightly polar (chloroform).

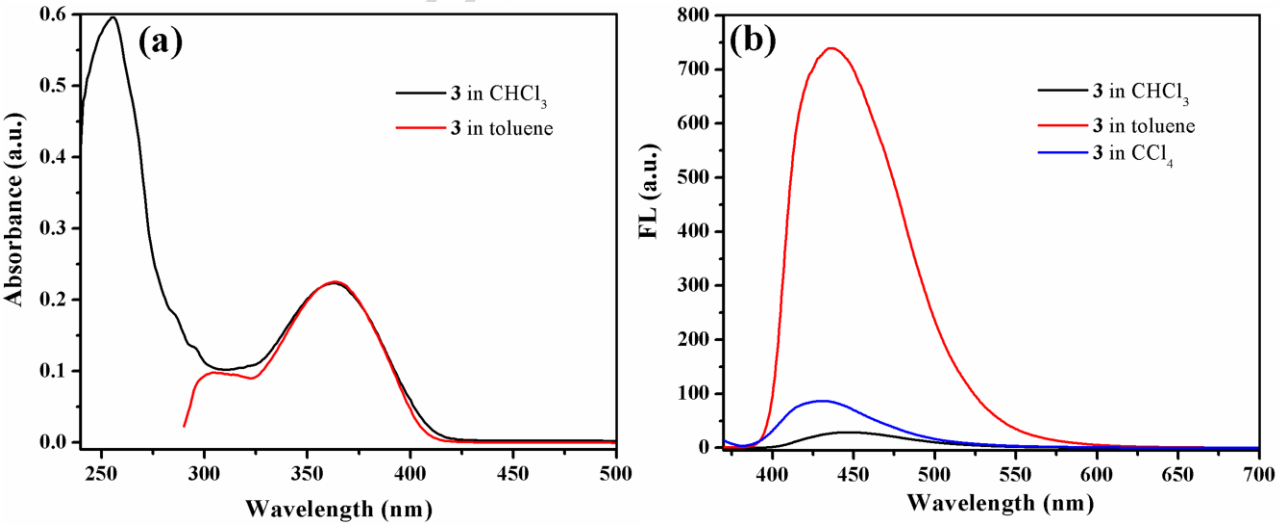


Figure 2. (a) Absorption and (b) emission ($\lambda_{ex}$ = 365 nm) spectra of pyrazoline **3** (solution concentration is $5\times10^{-4}$ wt%). In order to have a measurable fluorescence intensity, the emission spectra in $CHCl_3$ and $CCl_4$ were recorded in special conditions.

The fluorescence spectrum of pyrazoline **3** (Fig. 2b) taken in toluene differs significantly from the one recorded in chloroform. Thus, at $\lambda_{ex}$ = 365 nm, the FL spectrum in both solvents showed only a single emission maximum at 450 nm. Surprisingly, the emission intensities were very different for each solution: the emission intensity was high in toluene (quantum yield of 75%) and almost negligible in chloroform (quantum yield lower than 15%). This result pointed out that chloroform had an important fluorescence quenching effect on pyrazoline **3**.

With the view to explain the almost complete quenching of the emission intensity of pyrazoline **3** in chloroform, which represents an unprecedented behavior for pyrazolines, a series of additional experiments have been designed and performed. In order to examine the emission spectra of pyrazoline **3** in solvents having diverse structures and physical properties, several solvents have been selected. First, the FL spectrum of compound **3** has been recorded in dimethylsulfoxide (DMSO), a highly polar solvent, and compared to the one recorded in toluene, which is a non-polar solvent. The results have shown that the polarity of the solvent has little influence of the emission of pyrazoline **3**, as only slight bathochromic and hyperchromic effects could be noticed for the emission spectrum recorded in DMSO (Fig. 3.). A significant bathochromic effect is usually induced by a highly polar solvent and is a consequence of the photoexcitation process leading to a reorientation of the solvent molecules in the proximity of the fluorophore. Subsequently, part of the energy of the excited molecules of the fluorophore is transferred to the solvent, resulting in a batochromic effect. Owing to the presence of two chromophores in the structure of pyrazoline **3**, the magnitude of the aforementioned effect in DMSO is small and the Stokes shift is only 25 nm. The explanation is that processes involving both chromophores such as a significant geometrical relaxation of the molecule in the excited state and the internal charge transfer require a substantial part of the transferred energy.

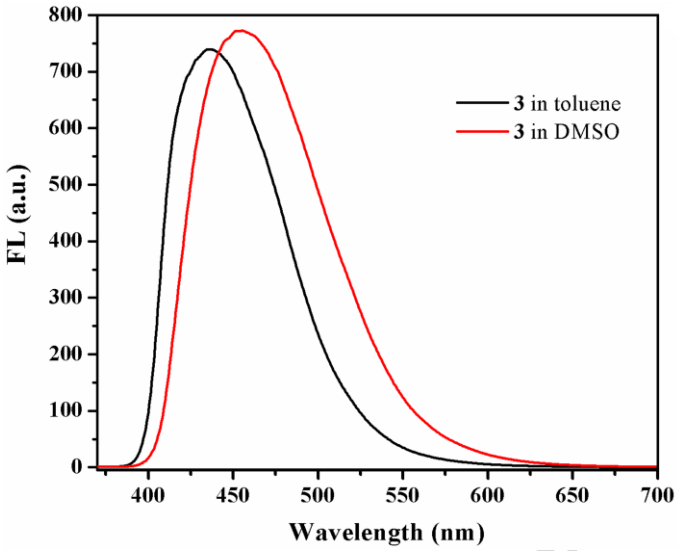


Figure 3. Fluorescence spectra of pyrazoline **3** in toluene (black line) and DMSO (red line); ($\lambda_{ex}$ = 365 nm).

Next, the emission spectrum of pyrazoline **3** was recorded in carbon tetrachloride, a solvent which is non-polar, but is structurally related to chloroform (Fig. 2b). The use of carbon tetrachloride in these experiments led again to an almost complete FL quenching, in a manner similar to that observed for the solutions of pyrazoline **3** in chloroform. Moreover, the fluorescence quenching was so intense in chloroform and carbon tetrachloride that, in order to evidence the small emission of pyrazoline **3**, these experiments have to be performed under conditions that allowed the amplification of the signal as described in the experimental part. These results strongly suggest that chloromethanes quench the fluorescence of pyrazoline **3**. Further research concerning this phenomenon has been made by studying the FL quenching effect of chloroform in pyrazoline **3** solutions in toluene. Thus, addition of increasing amounts of chloroform to a toluene solution of pyrazoline **3** resulted in a decrease of FL intensity, as shown in Figure 4. Although the same effect has been reported for compounds having different structures [27-29], it has been hitherto unknown for 1,3,5-triarylpyrazolines.

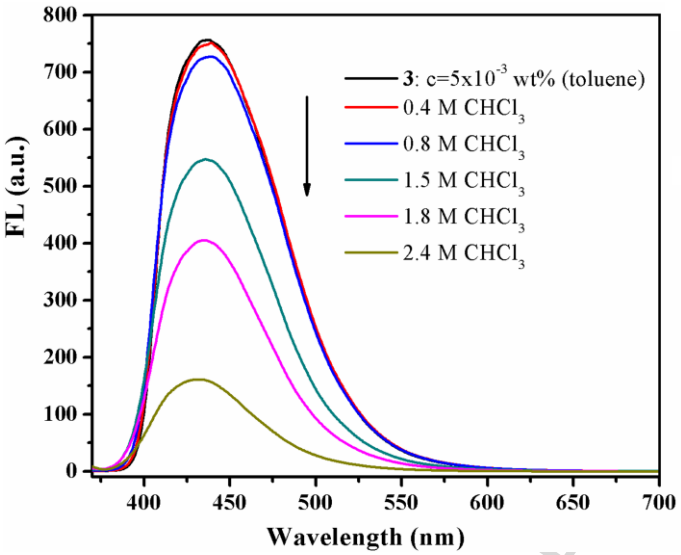


Figure 4. Fluorescence quenching effect of chloroform on the solution of pyrazoline **3** in toluene ($\lambda_{ex}$ = 365 nm).

Fluorescence quenching of a chromophore in the presence of halogenated alkanes is normally due to the formation of non-emissive exciplexes [27,30,31]. Generally, fluorescence quenching in such systems could be based either on a static mechanism, or a dynamic mechanism, or both. The static mechanism stipulates the formation of a charge transfer complex between the molecules of fluorophore in the excited state and those of the halogenated alkane. In contrast to the dynamic mechanism, the processes that are characterized by a static mechanism do not involve the diffusion of the molecules of the halogenated alkane towards the fluorophore. Valuable insight on the actual mechanism through which the fluorescence quenching of pyrazoline **3** by addition of chloroform in toluene solutions takes place can be gained from the chart in Figure 5 by using the Stern-Volmer equation. This chart has obtained by plotting the $I_0/I$ ratio as a function of the concentration of the quencher [Q].

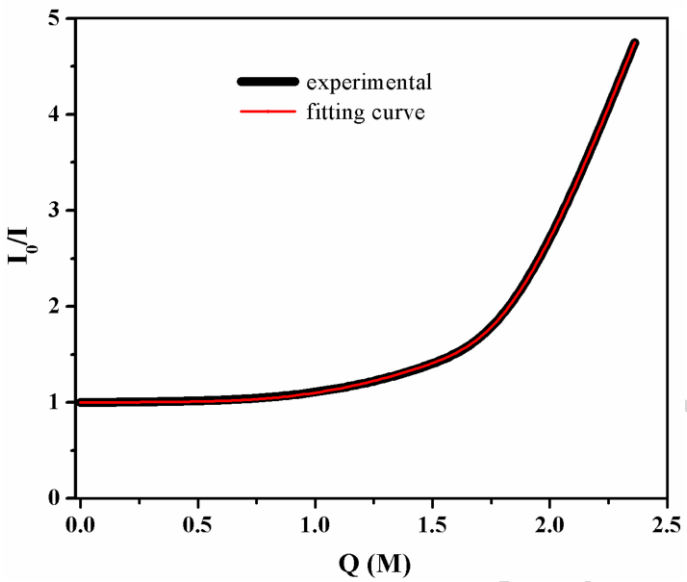


Figure 5. Fitting of the Stern-Volmer curve describing the nonlinear behavior of the fluorescence of pyrazoline **3** upon quenching with chloroform; $I_0$ represents the fluorescence intensity in the absence of the quencher, and I is the fluorescence intensity in the presence of the quencher's concentration [Q].

The dependence between $I_0/I$ and [Q] could be linear, and, in this case, the quenching takes place through a dynamic, collisional mechanism, which is largely controlled by diffusion. In our case, however, the chart obtained for the quenching of the fluorescence of pyrazoline **3** by chloroform exhibits a strong positive deviation (Fig. 5). The profile of the curve is typical for the situation in which the quenching occurs through a complex combination of both mechanisms. Thus, as some of the molecules in the excited state undergo a dynamic quenching through collisions, the rest of the fluorophore's molecules is deactivated instantaneously, as soon as they were excited. The static component of the quenching mechanism is the result of the presence of quencher molecules being randomly situated in the vicinity of the fluorophore's molecule as excitation occurs. One of the methods used to determine the contribution of the two mechanisms to the fluorescence quenching process consists in the calculation of the constants for dynamic and static quenching using the appropriate form of the Stern-Volmer equation. In our particular case, a modified Stern-Volmer equation [32] has been used, as follows:

$$I_0/I = 1+ Ksv[Q]exp(V[Q]),$$

where Ksv and V are the dynamic constant and the static constant, respectively.

The fitting of the experimental data onto the curve that has been generated using the above equation shows a perfect correlation between the theoretical model and experimental data (residual sum of squares, RSS = $3.4\times10^{-4}$), and, therefore, the calculation of the two constants using the modified Stern-Volmer equation is viable. The values obtained for these two constants (Ksv = $1.3\times10^{-2}$ $M^{-1}$; V = 2.033 $M^{-1}$) are indicative of a predominantly static quenching mechanism. Considering the excellent correlation between experimental data and the theoretical model, as well as the observation that the shift of the fluorescence intensity in the presence and absence of the quencher is insignificant, a plausible model for the fluorescence quenching process is the sphere-of-static action. This model presumes the existence of a defined volume inside which the whole quenching process takes place [33,34], and, according to this model, the size of the sphere can be estimated using the following equation:

$$v = 1000\ V/N = 4\pi r^3/3,$$

where N is Avogadro's number ($6.022\times10^{23}$/mole), and r is the radius of the sphere surrounding the fluorophore's molecule during fluorescence quenching.

In our case, the volume of the sphere can be calculated using the value of the static quenching constant (as determined with the modified Stern-Volmer equation):

$$v = 3\times1000\ V/N = 498.1\times10^{-23} = 4981\ Å^3, \text{ and}$$
$$r = [3 \times 4981/4\pi]^{1/3};\ r = 10.59\ Å$$

This value corresponds to a structure in which the molecules of chloroform are positioned preferentially on both sides of the plane that includes the aromatic ring of chromophore **C2**. The layout has been also confirmed by molecular modeling, as shown below.

Although the sphere-of-static action model fits perfectly the experimental data, this model cannot theoretically exclude the possibility of the presence of elements belonging to the dark complex model. This latter model assumes the formation of a particular type of complex between the fluorophore's molecules in the ground state and the quencher's molecules prior to excitation [35]. This specific type of complex does not imply a physical contact between the molecules involved in its formation, but rather a positioning of the

quencher's molecules close to the fluorophore's molecule as the result of subtle interactions between the two constituents of the complex. In this case, the unbound fluorophore is the source of fluorescence, and, according to this model, V is rather an association constant. The contribution of the dark complex model to the fluorescence quenching mechanism of pyrazoline **3** is justified by the existence of a minor tendency for the fluorescence intensity to shift towards lower wavelength numbers with the significant increase of the quencher's concentration. Therefore, although the noticeable effect is extremely weak, it may be potentially explained by a static quenching due to the presence of a slight association between the fluorophore and the quencher similar to that in dark complexes.

The essential characteristics of the particular electronic structure that was created by joining in a non-conjugated manner the two chromophores **C1** and **C2** within the molecule of pyrazoline **3** can be detailed with the help of the molecular model generated for this compound by quantum chemical methods (details in ESI - Pyrazoline **3** molecular model). The generation of a molecular model capable to reflect adequately the structure of the pyrazoline **3** has relied greatly on the information gleaned from the single crystal X-ray experiment.

Details regarding geometry optimization and full description of the method are presented in ESI (Table S2 and Fig. S2). Thus, the DFT methods B3LYP and CAM-B3LYP were employed for geometry optimization of pyrazoline **3** (Fig. 6). A comparison between the X-ray measured and predicted geometries indicated the best method in terms of root-mean-square-deviation (RMSD).

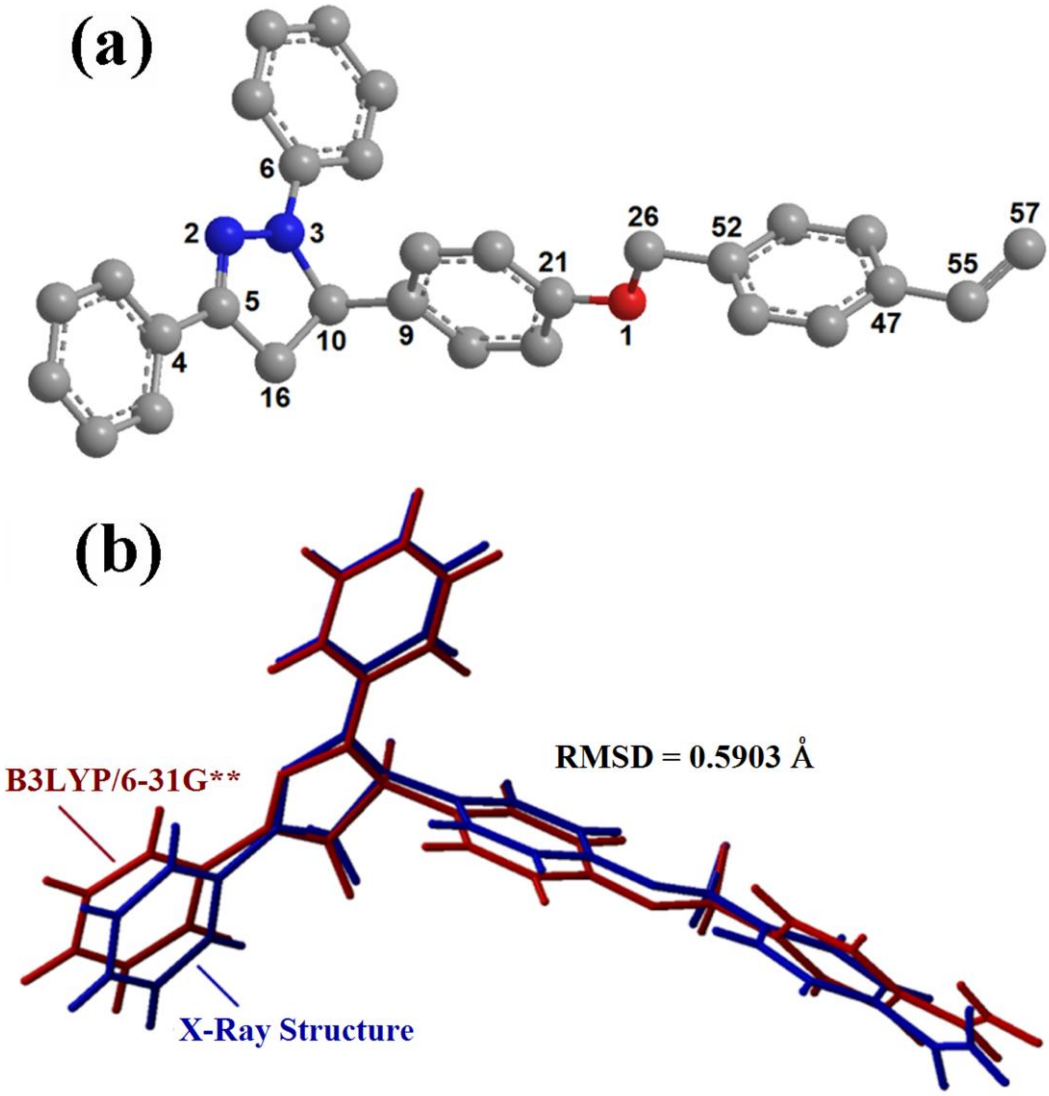


Figure 6. (a) Optimal geometry computed by DFT method at B3LYP/6-31G** level in ground state. (b) Superposition of molecular structures of pyrazoline **3**, X-ray structure (blue) and theoretical structures (red) computed by B3LYP/6-31G** (RMSD=0.5903 Å).

In the next step, the molecule geometry was calculated using the methodology for ***explicit*** solvents [36]. The geometries were validated by comparison of the computed electronic spectra with the experimental ones [37,38]. Thus, the predicted absorption maxima of 363.9 nm for chloroform and 356.2 nm for toluene were in good agreement with the experimental ones.

Then, the theoretical UV-Vis spectra were simulated in chloroform and toluene as ***implicit*** solvents using the polarizable continuum model (PCM) with the integral equation

formalism (IEFPCM) [39]. The best results were obtained when the theoretical spectra were predicted using CAM-B3LYP/6-31G** (Fig. 7).

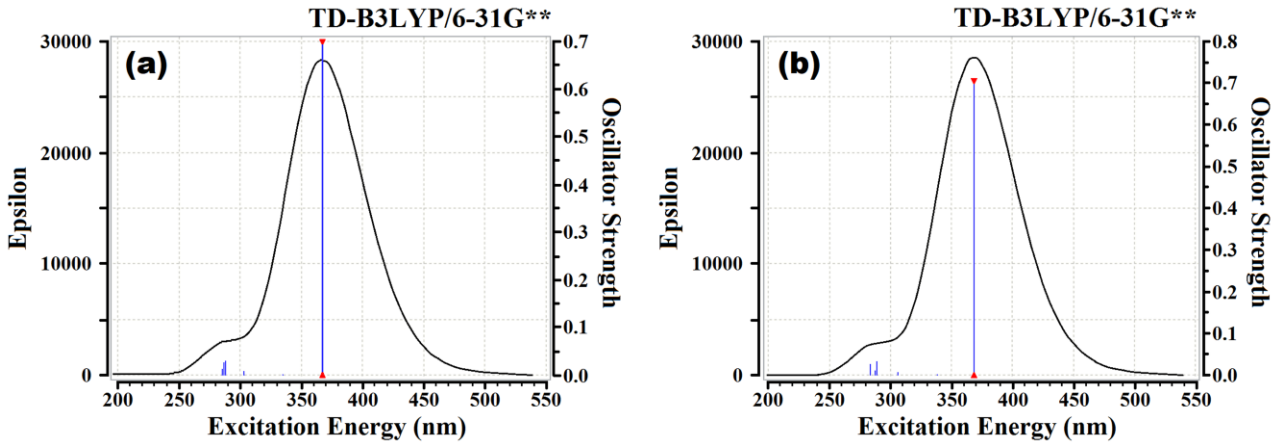


Figure 7. The electronic absorption spectrum computed by TD-DFT method at CAM-B3LYP/6-31G** level using IEFPCM model for implicit solvents: (a) chloroform and (b) toluene.

The molecular orbital analysis showed that the main contribution (52-53%) to the 242 nm transition represented the HOMO-2 → LUMO+1 electronic configuration. The lobes of these molecular orbitals (HOMO-2 and LUMO+1) were mainly spread onto the vinylbenzyloxy moiety **C2** (Fig. 8).

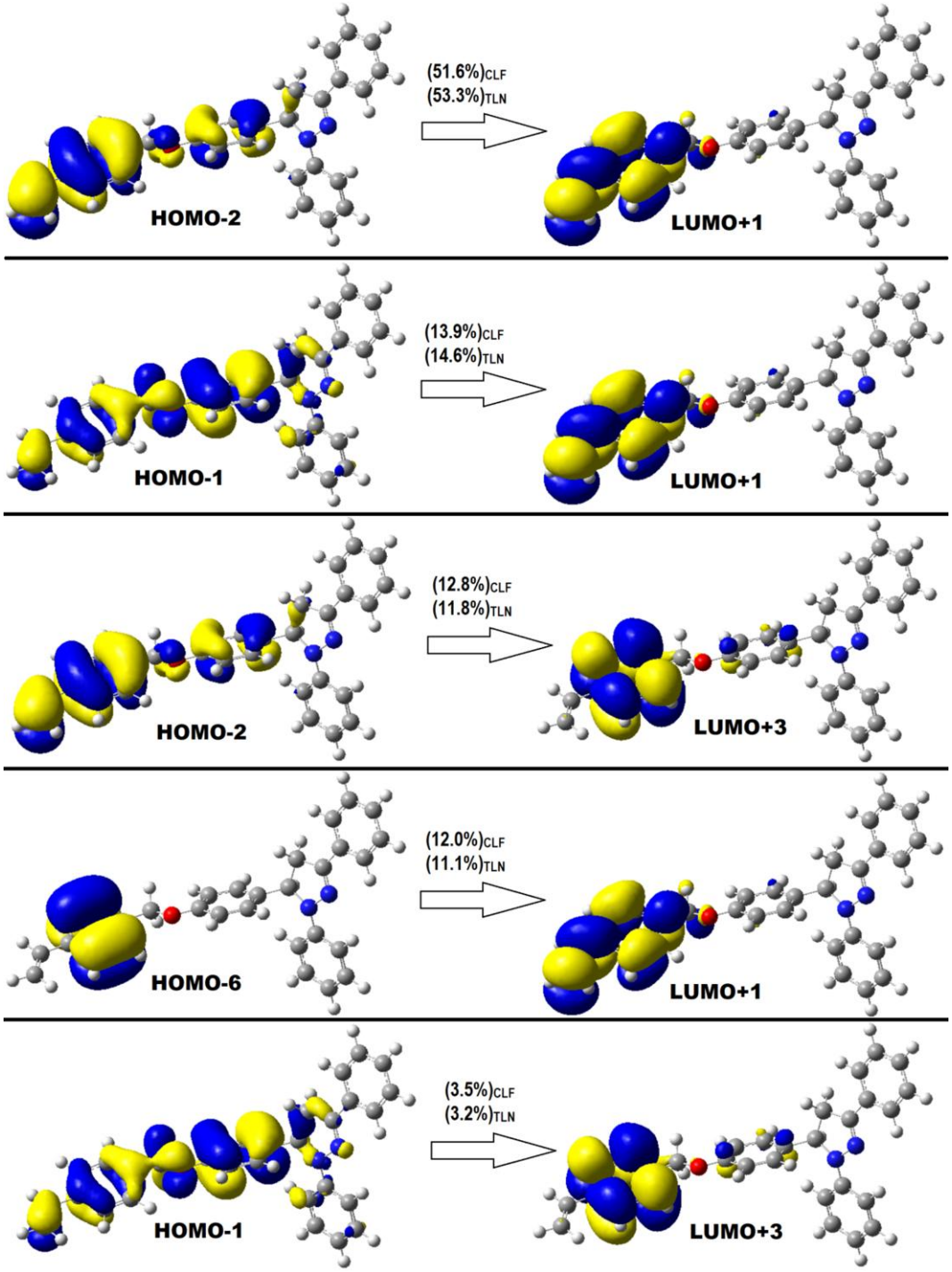


Figure 8. Molecular orbitals involved in the transition at the excitation energy of 242 nm along with assignments and percentage contributions; computation done at CAM-B3LYP/6-31G** level of theory.

Under the influence of explicit solvents, the lobes of HOMO are also distributed throughout the **C1** moiety in both solvents (Fig. 9). In toluene, most of the LUMO pattern is also located on **C1**, with no conjugation to the second **C2** chromophore (Fig. 9b). On the

other hand, in the case of chloroform, the lobes of LUMO are delocalized on both C1 and the adjacent chloroform molecule (Fig. 9a).

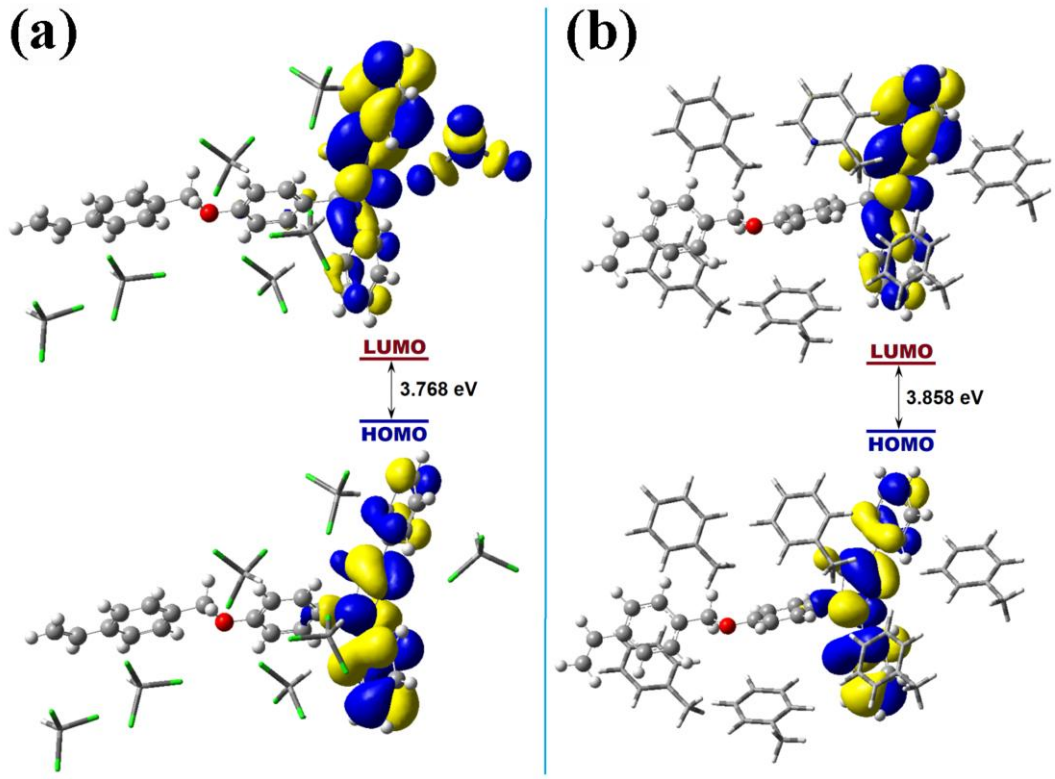


Figure 9. Patterns of frontier molecular orbitals (HOMO-LUMO) for pyrazoline **3** influenced by the presence of explicit solvent molecules (nearby SAS): (a) the effect of chloroform solvent and (b) the effect of toluene solvent.

All these calculations indicate that the presence of vinylbenzyloxy moiety **C2** in pyrazoline **3** generate structural particularities that lead to optical and electronic properties strongly influenced by the presence of neighbouring chloroform molecules. This observation sustains the hypothesis and mechanism concerning the fluorescence quenching by chloromethanes.

## Conclusions

A fluorescent pyrazoline having a vinyl moiety has been synthesized with the intention to develop new fluorescence sensors. For this purpose 4-vinylbenzyl chloride was reacted with 4-hydroxybenzaldehyde under the conditions of Williamson ether synthesis. Next, Claisen-Schmidt condensation of the resulting vinyl-containing aldehyde with acetophenone afford

the intermediate chalcone, which led to the desired pyrazoline **3** upon condensation with phenylhydrazine in acetic acid. The bichromophoric nature of this compound and the presence of the 4-vinylbenzyl)oxy]phenyl moiety are structural particularities that lead to specific fluorescence properties. Thus, the study of the optical properties in various solvents showed that the fluorescence of pyrazoline **3** is selectively quenched by chloroalkanes. The fluorescence quenching mechanism was analyzed considering chloroform as quencher. Stern-Volmer equation plot indicates a complex quenching mechanism with a strong static component. Molecular modeling of pyrazoline 3 was used to give details related to the cause of the fluorescence quenching by chloromethanes. Advanced computational techniques evidenced that, a non-radiative relaxation of the excited pyrazoline 3 is possible due to the formation of a specific HOMO-LUMO molecular orbital configuration that involves the chloromethane surrounding molecules. The fluorescence and bioactive properties of pyrazoline 3 have a high potential utility in development of sensors for detection and treatment of specific medical illness.

**Acknowledgement**

The computational chemistry section of the manuscript is part of a project that has received funding from the European Union's Horizon 2020 research and innovation program under the grant agreement N$^{o}$ 667387 WIDESPREAD 2-2014 SupraChem Lab.

A.L. Chibac is thankful for the financial support offered by CNCSIS-UEFISCDI, project number PN-III-P1-1.1-TE-2016-1390 (No. 34/2018).

**References**

[1] D.T. Simon, S. Kurup, K.C. Larsson, R. Hori, K. Tybrandt, M. Goiny, E.W.H. Jager, M. Berggren, B. Canlon, A. Richter-Dahlfors, Organic electronics for precise delivery of neurotransmitters to modulate mammalian sensory function, Nat. Mater. 8 (2009) 742–746.

[2] M. Barbaro, A. Caboni, P. Cosseddu, G. Mattana, A. Bonfiglio, Active devices based on organic semiconductors for wearable applications, IEEE Trans. Inf. Technol. Biomed. 14 (2010) 758–766.

[3] R.D. Jansen-van Vuuren, A. Armin, A.K. Pandey, P.L. Burn, P. Meredith, Organic photodiodes: the future of full color detection and image sensing, Adv. Mater. 28 (2016) 4766-4802.

[4] O. Tagit, N. Hildebrandt, Fluorescence sensing of circulating diagnostic biomarkers using molecular probes and nanoparticles, ACS Sens. 2 (2017) 31–45.

[5] K. Kikuchi, Design, synthesis, and biological application of fluorescent sensor molecules for cellular imaging, Adv. Biochem. Eng. Biotechnol. 119 (2010) 63-78.

[6] A.L. Chibac, M. Simionescu, G. Sacarescu, E.C. Buruiana, L. Sacarescu, New dansyl labeled polysilane: synthesis, characterization and sensor application, Eur. Polym. J. 95 (2017) 82-92.

[7] M.F. Khan, M.M. Alam, G. Verma, W. Akhtar, M. Akhter, M. Shaquiquzzaman, The therapeutic voyage of pyrazole and its analogs: a review, Eur. J. Med. Chem. 120 (2016) 170-201.

[8] M. Wanga, J. Zhanga, J. Liua, C. Xub, H. Juc, Intramolecular energy and charge transfer in 5-(9-anthryl)-3-(4-nitrophenyl)-1-phenyl-2-pyrazoline, J. Lumin. 99 (2002) 79–83.

[9] M. Sun, T. Pullerits, P. Kjellberg, W.J.D. Beenken, K. Han, Control of emission by intermolecular fluorescence resonance energy transfer and intermolecular charge transfer, J. Phys. Chem. A 110 (2006) 6324–6328.

[10] D.E. Rivett, J. Rosevear, J.F.K. Wilshire, The preparation and spectroscopic properties of some di- and tri-substituted 1,3,5-triphenyl-2-pyrazolines and related 2-pyrazolines, Aust. J. Chem. 36 (1983) 1649-1658.

[11] P.F. Wang, N. Onozawa-Komatsuzaki, Y. Himeda, H. Sugihara, H. Arakawa, K. Kasuga, 3-(2-Pyridyl)-2-pyrazoline derivatives: novel fluorescent probes for $Zn^{2+}$ ion, Tetrahedron Lett. 42 (2001) 9199–9201.

[12] H.B. Shi, S.J. Ji, B. Bian, Studies on transition metal ions recognition properties of 1-(2-benzothiazole)-3-(2-thiophene)-2-pyrazoline derivatives, Dyes Pigments 73 (2007) 394–396.

[13] CrysAlis RED, Oxford Diffraction Ltd., Version 1.171.36.32, 2003.

[14] O.V. Dolomanov, L.J. Bourhis, R.J. Gildea, J.A.K. Howard, H. Puschmann, OLEX2: a complete structure solution, refinement and analysis program, J. Appl. Cryst. 42 (2009) 339–341.

[15] G.M. Sheldrick, A short history of SHELX, Acta Cryst. A64 (2008) 112–122.

[16] Expanding the limits of computational chemistry, 09. Gaussian. Inc., Wallingford CT. http://www.gaussian.com/, 2009.

[17] R. Dennington, T. Keith, J. Millam, GaussView, Version 5, Semichem Inc., Shawnee Mission, KS., 2009**.**

[18] (a) YASARA official site (Yet Another Scientific Artificial Reality Application) http://www.yasara.org.; (b) E. Krieger, G. Vriend, YASARA View - molecular graphics for all devices - from smartphones to workstations, Bioinformatics 30 (2014) 2981-2982.

[19] Y. Qi, N. Li, X. Xia, J. Ge, J. Lu, Q. Xu, Synthesis of a fluorescent chemosensor based on a new copolymer containing multi-fluorophore, Mater. Chem. Phys. 124 (2010) 726–731.

[20] P.-Y. Gu, C.-J. Lu, Q.-F. Xu, G.-J. Ye, W.-Q. Chen, X.-M. Duan, L.-H. Wang, J.-M. Lu, Star-shaped polymer PFStODO by atom transfer radical polymerization: its synthesis, characterization, and fluorescence property, J. Polym. Sci. Part A: Polym. Chem. 50 (2012) 480–487.

[21] C. Yang, J. Xu, Y. Zhang, Y. Li, J. Zheng, L. Liang, M. Lu, Efficient monochromatic red-light-emitting PLEDs based on a series of nonconjugated Eu-polymers containing a neutral terpyridyl ligand, J. Mater. Chem. C 1 (2013) 4885–4901.

[22] V. Erapalapati, N. Madhavan, Versatile soluble oligomeric styrene supports for peptide synthesis, J. Polym. Sci. Part A: Polym. Chem. 53 (2015) 2501–2509.

[23] L. Wu, P. Wang, C. Zhang, J. He, D. Chen, J. Jun, Q. Xu, J. Lu, Adjusting the proportion of electron-withdrawing groups in a graft functional polymer for multilevel memory performance, Chem. Asian J. 11 (2016) 102–111.

[24] Q. Yu, L. Najun, X. Qingfeng, G. Jianfeng, X. Xuewei, L. Jianmei, Synthesis and characterization of a new amphiphilic copolymer containing multihydroxyl segments for drug carrier, J. Appl. Polym. Sci. 121 (2012) 2843–2850.

[25] H.H. Pham, C. Szent-Gyorgyi, W.L. Brotherton, B.F. Schmidt, K.J. Zanotti, A.S. Waggonera, B.A. Armitage, Bichromophoric dyes for wavelength shifting of dye-protein fluoromodules, Org. Biomol. Chem. 13 (2015) 3699-3710.

[26] T. Papalia, A. Barattucci, S. Campagna, F. Puntoriero, T. Salerno, P. Bonaccorsi, Synthesis and photophysical properties of a bichromophoric system hosting a disaccharide spacer, Org. Biomol. Chem. 15 (2017) 8211–8217.

[27] P.K. Beherab, T. Mukherjeec, A.K. Mishra, Quenching of substituted naphthalenes fluorescence by chloromethanes, J. Lumin. 65 (1995) 137- 142.

[28] D. Goswami, R.S. Sarpal, S.K. Dogra, Fluorescence quenching of few aromatic amines by chlorinated methanes, Bull. Chem. Soc. Jpn. 64 (1991) 3137-3141.

[29] J. Sujatha, A.K. Mishra, Fluorescence quenching of naphthalene and its substitutions by chloroethanes and –ethylenes, J. Lumin. 75 (1997) 135-141.

[30] D.A. Labianca, G.N. Taylor, G.S. Hammond, Structure-reactivity factors in the quenching of fluorescence from naphthalenes by conjugated dienes, J. Am. Chem. Soc. 94 (1972) 3679–3683.

[31] S.L. Mattes, S. Farid, Exciplexes and electron transfer reactions, Science 226 (1984) 917-921.

[32] M.R. Eftink, C.A. Ghiron, Fluorescence quenching of indole and model micelle systems, J. Phys. Chem. 80 (1975) 486–493.

[33] T. Moriya, Excited-state reactions of coumarins in aqueous solutions. II. The fluorescence quenching of 7-ethoxycoumarins by halide ions, Bull. Chem. Soc. Jap. 57 (1984) 1723-1730.

[34] R. Roy, S. Mukherye, Fluorescence quenching of carbazole and indole by ethylenetrithiocarbonate, Chem. Phys. Lett. 140 (1987) 210-214.

[35] H. Boaz, G.K. Roiiefson, The quenching of fluorescence. Deviations from the Stern-Volmer law, J. Am. Chem. Soc. 72 (1950) 3435-3443.

[36] A. Airinei, D.L. Isac, M. Homocianu, C. Cojocaru, C. Hulubei, Solvatochromic analysis and DFT computational study of an azomaleimide derivative, J. Mol. Liq. 240 (2017) 476-485.

[37] S. Grimme, Calculation of the electronic spectra of large molecules, Rev. Comput. Chem. 20 (2004) 153–218.

[38] S. Fleming, A. Mills, T. Tuttle, Predicting the UV–vis spectra of oxazine dyes, Beilstein J. Org. Chem. 7 (2011) 432–441.

[39] J.B. Foresman, Æ. Frish, Exploring chemistry with electronic structure methods, second ed., Gaussian, Inc., Pittsburgh, 1996.

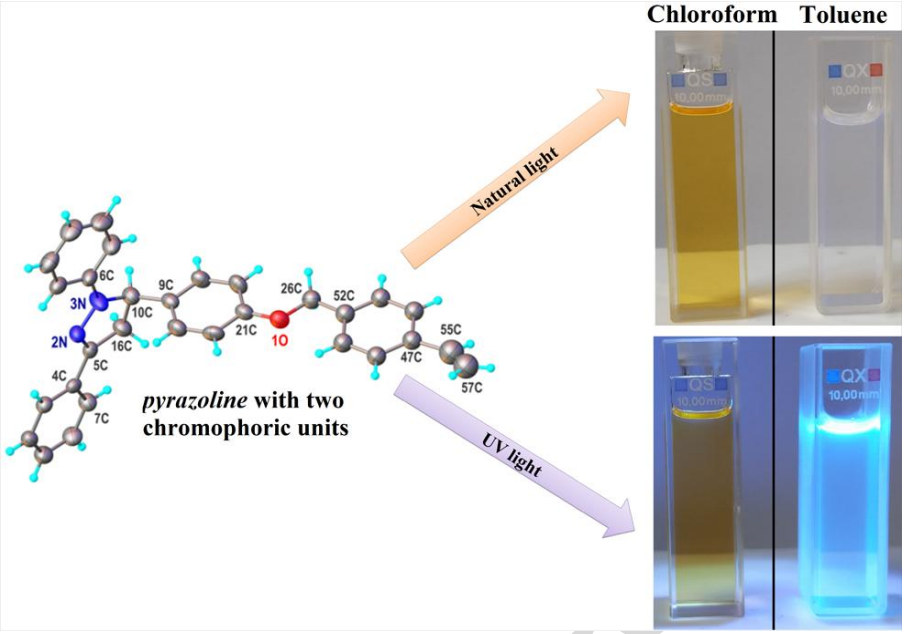


Graphical abstract

**Highlights**

- fluorescence quenching of pyrazoline derivative by chloroalkanes.
- synthesis of aryl trisubstituted pyrazoline with two non-conjugated chromophoric units.
- structural and optical particularities
- the fluorescence quenching mechanism.
- molecular modeling of pyrazoline by Density Functional Theory in implicit solvents.